Hazem. I. Ali
Control & Systems Engineering Department, University of Technology, Baghdad, Iraq.
60143@uotechnology.edu.iq

Zain. M. Shareef
Control & Systems Engineering Department, University of Technology, Baghdad, Iraq.
Eng.zaincontrol1991@gmail.com

Received on: 23/05/2017
Accepted on: 24/05/2018
Published online" 25/10/2018

Full State Feedback H_2 and H-infinity Controllers Design for a Two Wheeled Inverted Pendulum System

Abstract *- In this work, two robust controllers, which are full state feedback, H_2 and full state feedback H_∞ controllers are proposed for the two wheeled inverted pendulum system. The nonlinear equations for the two wheeled inverted pendulum system are developed using Euler – Lagrange equation. The system parameters changes are considered to show the effectiveness of the proposed robust controllers. These controllers are proposed not only to stabilize the pendulum in upright position but also to drive the position to track a given reference input. The results show that more desirable robustness and time response specifications can be achieved using the proposed controllers. The effectiveness of the proposed controllers is verified experimentally using real two wheeled inverted pendulum system.*

Keywords *- Robust control, Two wheeled inverted pendulum, H_2 full state feedback control, optimal control, H_∞ controller.*

How to cite this article: H.I. Ali and Z.M. Shareef, "Full State Feedback H_2 and H infinity Controllers Design for a Two Wheeled Inverted Pendulum System," *Engineering and Technology Journal*, Vol. 36, Part A, No. 10, pp. 1110-1121, 2018.

1. Introduction

Since it is flexible and efficient in many industrial operations, the two-wheeled inverted pendulum is considered one of very important [1]. It has a possible application chance in many fields, such as medical applications, laboratory illustrations, military applications, automation industries, aerospace applications, space industry and entertaining applications. The features of the two-wheeled inverted pendulum systems, which make them attractive for users, are: no need of fuels, high ease of use and great maneuverability because of independent control of two wheels and lower cost of energy than fuels. The problems of this kind of systems are unstable, nonlinear, nonholonomic constraint and under actuated. The control of the under actuated system becomes more discomfort for the researchers to resolve. The under actuated system is a category of systems where the control inputs are less than DOFs to be stabilized. For the two wheeled inverted pendulum system, there are only two inputs (torque) from the motors installed to the two wheels, but there are three DOFs, which are position system, pendulum angle and rotating angle of the system. Further, the two-wheeled system is a MIMO system where the two inputs might directly control the three outputs and it is essentially a nonminimum phase system. Further, the variation in system parameters causes an uncertainty in a number of model's parameters and leads to variation in system dynamics [2]. Several researches have been introduced for developing a mathematical model and control of the two wheeled inverted pendulum system. Newton-Euler equations of motion and Euler Lagrange method are the most used methods [3]. On the other hand, different control approaches have been proposed to control this system, for instance, Sliding Mode Control (SMC)[4], LQR Controller [5], Adaptive Sliding Mode Control [2] and Back stepping Control [6]. The robust control is one of the important techniques that are used to stabilize the plant and achieve an acceptable performance in the presence of disturbance, noise, unmodelled plant dynamics and plant parameters uncertainties. Further, when a linearized model is used to represent a nonlinear plant, a model plant mismatch may be occurred and in this case, a robust control becomes a need [7, 8]. In this paper, the model of the two wheeled inverted pendulum system is obtained by Euler equations of motion. The full state feedback controller is designed using H_2 and H_∞ approaches to achieve the required robustness in stability and performance.

https://doi.org/10.30684/etj.36.10A.12
2412-0758/University of Technology-Iraq, Baghdad, Iraq

2. System Modeling

The dynamic modeling of the two wheeled inverted pendulum system includes deriving the equations of motion using Euler Lagrange method, determining the nonlinear state-space model, assigning suitable state space variables and obtaining the linear model from the nonlinear model. Figure 1 shows the schematic diagram of the two-wheeled inverted pendulum system [9]. It is shown that the system has three degrees of freedom *i.e.* about the X, Y and Z axis. The angles are illustrated for the wheeled inverted pendulum system in Figure 1. The rotation around the lateral axis X is known as roll and the rotation around the vertical axis Y is known as yaw and the rotation around the lateral axis Z is known as pitch [10]. The Lagrangian is the difference between system's kinetic and potential energies. The Lagrangian function of the system is described by [11]:

$$L = E - V \quad (1)$$

where E is the total kinetic energy of the system and V is the total potential energy of the system. The next step is to put L from the Lagrangian function into the Lagrangian equation. The Euler Lagrange equation of motion for the system is given by [3]:

$$\frac{\partial}{\partial t}\left(\frac{\partial L}{\partial \dot{x}}\right) - \frac{\partial L}{\partial x} = F_i \quad (2)$$

$$\frac{\partial}{\partial t}\left(\frac{\partial L}{\partial \dot{\phi}}\right) - \frac{\partial L}{\partial \phi} = F_i \quad (3)$$

$$\frac{\partial}{\partial t}\left(\frac{\partial L}{\partial \dot{\psi}}\right) - \frac{\partial L}{\partial \psi} = F_i \quad (4)$$

where F_i represents the forced function of the system, (x, ϕ, ψ) represent generalized states for the system.

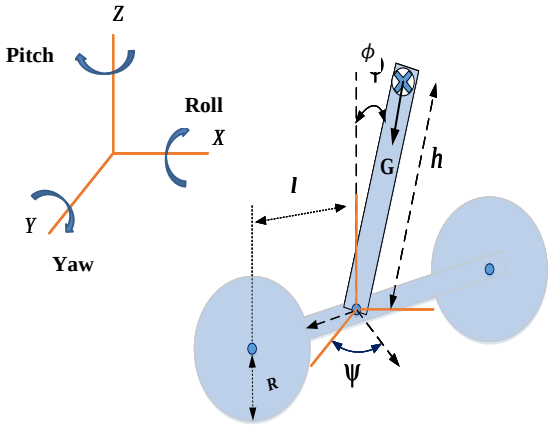

Figure 1: The two wheeled inverted pendulum structure [18]

Total kinetic energy for the two wheeled inverted pendulum system is [11]:

$$E = \frac{1}{2} M_b \left[\dot{x}^2 + 2h\,\dot{x}\,\dot{\phi}\,cos\phi + h^2\,\dot{\phi}^2 + h^2\,\dot{\psi}^2 \sin^2\phi\right] + \frac{1}{2}\left[I_x\dot{\phi}^2 + I_y\dot{\psi}^2 sin^2\phi + I_z\dot{\psi}^2 cos^2\phi\right] + \frac{1}{2}(M_w + \frac{I_a}{R^2})(\dot{x}^2 + l\dot{\psi}^2) \quad (5)$$

where M_b is the mass of body (Kg), I_x is the moment of inertia of body x-axis (Kgm^2), I_y is the moment of inertia of body y-axis (Kgm^2), I_z is the moment of inertia of body z-axis (Kgm^2), M_w represents the mass of each wheel (Kg), R represents the radius of each wheel (m), l represents the distance between the wheels (m), θ represents angle of wheel $(degree)$ and I_a is the moment of inertia of wheel about the center (Kgm^2).

Total potential energy V is;

$$V = M_b g h\, cos\phi + M_b g R \quad (6)$$

where g is the acceleration due to gravity (ms^{-2}). The total energy L in equation (1) is given by:

$$L = \left[\frac{M_b}{2} + M_w + \frac{I_a}{R^2}\right]\dot{x}^2 + \left[M_b h^2 + \frac{1}{2}I_x\right]\dot{\phi}^2 + M_b h cos\phi\,\dot{x}\dot{\phi} - [M_b g h cos\phi + M_b g R] + \left[\left(M_w + \frac{I_a}{R^2}\right)l^2 + \frac{1}{2}\left(I_y sin^2\phi + I_z cos^2\phi + M_b h sin^2\phi\right)\right]\dot{\psi}^2 \quad (7)$$

By partial differentiation of the equation (7) for each of $(\dot{x}, \dot{\phi}, \dot{\psi})$ then, To linearize the nonlinear equations that describe the two wheeled inverted pendulum system, the Jacobian method is used as follows [12]:

$$\ddot{\phi}(t) = \frac{[M_b R^2 + 2M_w R^2 + 2I_a]M_b g h}{[(M_b + 2M_w)R^2 + 2I_a]I_x + 2M_b h^2(M_w R^2 + I_a)}\phi(t) - \frac{[M_b R^2 + 2M_w R^2 + 2I_a] + M_b h R}{[(M_b + 2M_w)R^2 + 2I_a]I_x + 2M_b h^2(M_w R^2 + I_a)}(T_1 + T_2) \quad (8)$$

$$\ddot{x}(t) = -\frac{M_b^2 g R^2 h^2}{(M_b h^2 + I_x)[(M_b + 2M_w)R^2 + 2I_a] - (M_b R h)^2}\phi(t) + \frac{R(M_b h^2 + M_b h R + I_x)}{(M_b h^2 + I_x)[(M_b + 2M_w)R^2 + 2I_a] - (M_b R h)^2}(T_1 + T_2) \quad (9)$$

$$\ddot{\psi}(t) = \frac{l}{R\left[2\left(M_w + \frac{I_a}{R^2}\right)l^2 + I_z\right]}(T_1 - T_2) \quad (10)$$

Equations (8), (9) and (10) are linearized about the operating state. The obtained linearized model is:

$$\begin{bmatrix}\dot{x}(t)\\ \ddot{x}(t)\\ \dot{\psi}(t)\\ \ddot{\psi}(t)\\ \dot{\phi}(t)\\ \ddot{\phi}(t)\end{bmatrix}=\begin{bmatrix}0&1&0&0&0&0\\0&0&0&0&-a_1&0\\0&0&0&1&0&0\\0&0&0&0&0&0\\0&0&0&0&0&1\\0&0&0&0&a_2&0\end{bmatrix}\begin{bmatrix}x(t)\\ \dot{x}(t)\\ \psi(t)\\ \dot{\psi}(t)\\ \phi(t)\\ \dot{\phi}(t)\end{bmatrix}+\begin{bmatrix}0&0\\b_1&b_2\\0&0\\b_3&-b_4\\0&0\\-b_5&-b_6\end{bmatrix}\begin{bmatrix}T_1\\T_2\end{bmatrix} \quad (11)$$

$$\begin{bmatrix}x(t)\\ \psi(t)\\ \phi(t)\end{bmatrix}=\begin{bmatrix}1&0&0&0&0&0\\0&0&1&0&0&0\\0&0&0&0&1&0\end{bmatrix}\begin{bmatrix}x(t)\\ \dot{x}(t)\\ \psi(t)\\ \dot{\psi}(t)\\ \phi(t)\\ \dot{\phi}(t)\end{bmatrix}+D\begin{bmatrix}T_1\\T_2\end{bmatrix} \quad (12)$$

where

$$a_1=\frac{M_b^2gR^2h^2}{(M_bh^2+I_x)[(M_b+2M_w)R^2+2I_a]-(M_bRh)^2}$$

$$a_2=\frac{[M_bR^2+2M_wR^2+2I_a]M_bgh}{[(M_b+2M_w)R^2+2I_a]I_x+2M_bh^2(M_wR^2+I_a)}$$

$$b_1=\frac{R(M_bh^2+M_bhR+I_x)}{(M_bh^2+I_x)[(M_b+2M_w)R^2+2I_a]-(M_bRh)^2}$$

$$b_2=\frac{R(M_bh^2+M_bhR+I_x)}{(M_bh^2+I_x)[(M_b+2M_w)R^2+2I_a]-(M_bRh)^2}$$

$$b_3=\frac{l}{R\left[2\left(M_w+\frac{I_a}{R^2}\right)l^2+I_z\right]}$$

$$b_4=\frac{l}{R\left[2\left(M_w+\frac{I_a}{R^2}\right)l^2+I_z\right]}$$

$$b_5=\frac{[M_bR^2+2M_wR^2+2I_a]+M_bhR}{[(M_b+2M_w)R^2+2I_a]I_x+2M_bh^2(M_wR^2+I_a)}$$

$$b_6=\frac{[M_bR^2+2M_wR^2+2I_a]+M_bhR}{[(M_b+2M_w)R^2+2I_a]I_x+2M_bh^2(M_wR^2+I_a)}$$

Table 2.1 lists the nominal parameters of the real two wheeled inverted pendulum system.

Table 2.1: System nominal parameters.

Symbol	Value	Unit
M_b	0.502	Kg
M_w	0.054	Kg
h	0.31	m
R	0.065	m
l	0.18	m
I_x	9.1196×10^{-4}	Kgm^2
I_z	6.693×10^{-3}	Kgm^2
I_a	2.851585×10^{-5}	Kgm^2
g	9.81	ms^{-2}

3. System Set up

In this section, the different components of the real two-wheeled inverted pendulum system are demonstrated. The two main parts of the system are the mobile robot and the inverted pendulum. Figure 2 shows the SainSmart InstaBots Upright Rover Kit V 3.0 Pro Updated 2 Wheel Self Balancing Robot Kit Mega 2560 which represents the mobile robot part [13]. To construct the two wheeled inverted pendulum system, we have connected a pendulum to the mobile robot body at the center of the chassis. The constructed mobile inverted pendulum system is shown in Figure 3.

Figure 2: SainSmart InstaBots Upright Rover Kit Wheel Self Balancing [22].

Figure 3: The constructed real two wheeled inverted pendulum system.

4. Controllers Design

In this section, the design of full state feedback controller using H_2 control and H_∞ control is presented. The main objective of the proposed controllers is to stabilize the mobile inverted pendulum system and achieve an acceptable robustness with a more desirable performance.

I. Statement of the Problem

Consider the linear time invariant control system expressed by:

$$\dot{x}(t)=Ax(t)+B_1\,d(t)+B_2\,u(t) \quad (13)$$

$$e(t)=C_1x(t)+D_{12}\,u(t) \quad (14)$$

$$y(t)=x(t) \quad (15)$$

where $x(t)\in R^n$ represents the state vector, $e(t)\in R^h$ represents the controlled output vector, $y(t)\in R^r$ represents the output, $u(t)\in R^n$ represents the control vector and $d(t)\in R^n$ represents the disturbance. For design requirements, it is necessary to assume that the the system matrix A is of full rank, the pairs (A,B_1) and (A,B_2) are stabilizable, and the pair (C_1,A) is detectable. Also, it is required that all state measurements can be made. Obtaining a scalar state feedback control is the main objective of this work. The state feedback control can be expressed as:

$$u(t) = K\,x(t) \quad (16)$$

where K is called the state feedback gain matrix.
The control law assigns the closed loop eigenvalues required to stabilize the system and achieve a desirable performance in the presence of disturbance and over a range of system parameters changes. Further, this work focuses on the system position and pendulum angle and the goal is to follow a predetermined input position with a minimum deviation in pendulum angle.

II. H_2 Controller

Assume that:

$$M = \begin{bmatrix} A & B_1 & B_2 \\ C_1 & 0 & D_{12} \\ I & 0 & 0 \end{bmatrix} \quad (17)$$

The block diagram of H_2 control is shown in Figure 4.

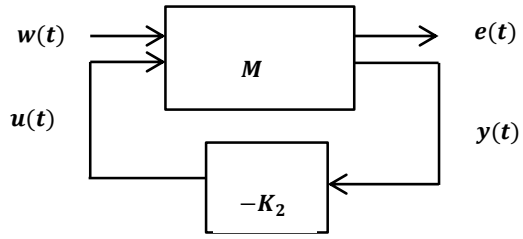

Figure 4: H_2 control block diagram[24].

where $w(t)$ represents the external inputs (set point, disturbance) [14].
The H_2 norm of the system error due to a white noise input is:

$$\|T_{ed}\|_{H_2}^2 = E(e^T(t)e(t)) \quad (18)$$

where T_{ed} is the transfer function from $d(t)$ to $e(t)$, then

$$e^T(t)e(t) = x(t)^T Q_f x(t) + 2x(t)^T N_f u(t) + u(t)^T R_f\, u(t) \quad (19)$$

where $Q_f = {C_1}^T C_1$, $N_f = {C_1}^T D_{12}$, $R_f = {D_{12}}^T D_{12}$.
Hence, the resulting cost function to be minimized is:

$$J = \int_{t_0}^{t_f} [\,x(t)^T Q_f x(t) + 2x(t)^T N_f u(t) + u(t)^T R_f\, u(t)]dt \quad (20)$$

And the optimal control action is expressed by:

$$u(t) = -K_2\, x(t) \quad (21)$$

where

$$K_2 = {R_f}^{-1}({B_2}^T P + {N_f}^T) \quad (22)$$

where P is symmetric and positive definite transformation matrix. It is determined using the following Riccati equation:

$$\left(A - B_2 {R_f}^{-1} {N_f}^T\right)^T P + P(A - B_2 {R_f}^{-1} {N_f}^T) - P B_2\, {R_f}^{-1} {B_1}^T P + Q_f - N_f\, {R_f}^{-1} {N_f}^T = 0 \quad (23)$$

III. Structured Uncertainty Construction

The robust control techniques are taking uncertainties methodically into account when designing a controller or when analyzing a control system. Model uncertainty is called "structured" when there is real parameter uncertainty in the model, or if there are multiple unstructured uncertainties located at various points within the system at the same time [15]. Consider the state space model block shown in Figure 5 and assume that

$$M = \begin{bmatrix} M_{11} & M_{12} \\ M_{21} & M_{22} \end{bmatrix} \quad (24)$$

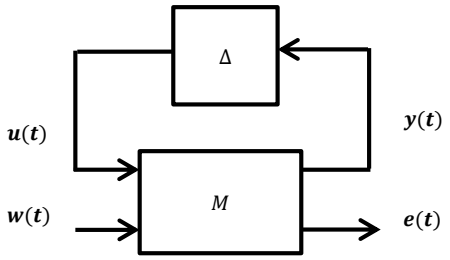

Figure 5: Block diagram of state space model [18].

The equation of upper linear fractional transformation (ULFT) can be expressed by [16, 17]:

$$F_u(M, \Delta) = M_{22} + M_{21}\Delta\ (I - M_{11}\Delta)^{-1} M_{12} \quad (25)$$

where $F_u(M, \Delta)$ is the upper linear fractional transformation of M and Δ. To obtain the (ULFT) representation of a state space model expressed by:

$$G(s) = D + C\,(sI - A)^{-1} B \quad (26)$$

The transfer function matrix $G(s)$ is compared to equation (25) to give:

$M_{22} = D, M_{21} = C, M_{11} = A, M_{12} = B$ and $\Delta = \frac{1}{s} I$

The system upper linear fractional transformation is shown in Figure 6.

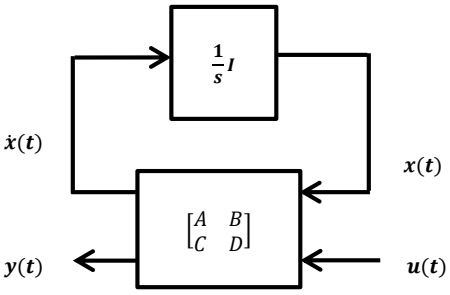

Figure 6: Block Diagram of system with upper linear fractional transformation [18].

Consider the uncertain linear system $(A_\delta, B_\delta, C_\delta \; and \; D_\delta)$ with k uncertain parameters $\delta_1, \dots, \delta_k$ and assume that

$$A_\delta = A_0 + \sum_{i=1}^{k} \delta_i \hat{A}_i \quad (27)$$

$$B_\delta = B_0 + \sum_{i=1}^{k} \delta_i \hat{B}_i \quad (28)$$

$$C_\delta = C_0 + \sum_{i=1}^{k} \delta_i \hat{C}_c \quad (29)$$

$$D_\delta = D_0 + \sum_{i=1}^{k} \delta_i \hat{D}_i \quad (30)$$

where $(A_0, B_0, C_0 \; and \; D_0)$ is the nominal matrices of the plant and k represents the number of variation parameters. The uncertain matrices $(\hat{A}_i, \hat{B}_i, \hat{C}_i \; and \; \hat{D}_i)$ are known, and they describe how uncertain parameters $\delta_1, \delta_2, \dots, \delta_k$ enter into the model. It will be assumed that there are n states, m inputs, p outputs [18].

Reformulating equations (27), (28), (29) and (30), the following equations are obtained:

$$N_\delta = \begin{bmatrix} A_0 + \sum_{i=1}^{k} \delta_i \hat{A}_i & B_0 + \sum_{i=1}^{k} \delta_i \hat{B}_i \\ C_0 + \sum_{i=1}^{k} \delta_i \hat{C}_i & D_0 + \sum_{i=1}^{k} \delta_i \hat{D}_i \end{bmatrix} \quad (31)$$

where N_δ represents A_δ, B_δ, C_δ and D_δ. The δ_i matrix can be defined as:

$$\delta_i = diag[\delta_{a_1}, \delta_{a_2}, \delta_{b_1}, \delta_{b_2}, \delta_{b_3}, \delta_{b_4}, \delta_{b_5}, \delta_{b_6}] \quad (32)$$

Reformulating equation (31), gives:

$$N_\delta = \begin{bmatrix} A_0 & B_0 \\ C_0 & D_0 \end{bmatrix} + \sum_{i=1}^{k} \delta_i p_i \quad (33)$$

where the p_i matrices are appropriately partitioned. The p_i matrices are found with the expansion for the uncertainty matrices having zero-order cross-product, and then rewriting equations (33) yields:

$$\delta_i p_i = \delta_{a_1} p_1 + \delta_{a_2} p_2 + \delta_{b_1} p_3 + \delta_{b_2} p_4 + \delta_{b_3} p_5 + \delta_{b_4} p_6 + \delta_{b_5} p_7 + \delta_{b_6} p_8 \quad (34)$$

The matrix p_i can be decomposed into the product of appropriately partitioned column and row matrices as follows:

$$p_i = \begin{bmatrix} H_i \\ W_i \end{bmatrix} [R_i^H \quad Z_i^H] = \begin{bmatrix} H_i \\ W_i \end{bmatrix} \delta_i I_{qi} [R_i^H \quad Z_i^H] \quad (35)$$

The rank of the matrix P_i is q_i and $H_i, W_i, R_i \; and \; Z_i$ are $n \times q_i, p \times q_i, n \times q_i$ and $m \times q_i$ matrix, respectively.

Substituting equation (35) into equation (33) yields:

$$N_\delta = \begin{bmatrix} A & B \\ C & D \end{bmatrix} + \begin{bmatrix} H_1 & \dots\dots & H_8 \\ W_1 & \dots\dots & W_8 \end{bmatrix} \begin{bmatrix} \delta_{a_1} I_{q1} & \cdots & 0 \\ \vdots & \ddots & \vdots \\ 0 & \cdots & \delta_{b_6} I_{q8} \end{bmatrix} \begin{bmatrix} R_1^H & Z_1^H \\ \vdots & \vdots \\ R_8^H & Z_8^H \end{bmatrix} \quad (36)$$

By comparison with equation (25), we obtain:

$$M_\delta = \begin{bmatrix} M_{11} & M_{12} \\ M_{21} & 0 \end{bmatrix} M_{11} = \begin{bmatrix} A & B \\ C & D \end{bmatrix}$$

$$M_{12} = \begin{bmatrix} H_1 & \dots\dots & H_8 \\ W_1 & \dots\dots & W_8 \end{bmatrix} \; M_{22} = 0$$

$$M_{21} = \begin{bmatrix} R_1^H & Z_1^H \\ \vdots & \vdots \\ R_8^H & Z_8^H \end{bmatrix} \Delta_p = \begin{bmatrix} \delta_{a_1} I_{q1} & \cdots & 0 \\ \vdots & \ddots & \vdots \\ 0 & \cdots & \delta_{b_6} I_{q8} \end{bmatrix} \quad (37)$$

where

$B_2 = [H_1 \quad \dots\dots\dots \quad H_8]$

$D_{12} = [W_1 \quad \dots\dots\dots \quad W_8]$

$C_2^H = [R_1^H \quad \dots\dots \quad R_8^H]$

$D_{21}^H = [Z_1^H \quad \dots\dots \quad Z_8^H]$

$D_{22} = 0$

Rewriting equation (46) gives:

$$M_\delta = \begin{bmatrix} A & B_{\delta 1} & B_2 \\ C & D_{11} & D_{\delta 12} \\ C_{\delta 2} & D_{\delta 21} & 0 \end{bmatrix} \quad (38)$$

IV. H_∞ Controller

A full state feedback H_∞ control is considered to stabilize and track the two wheeled inverted pendulum system and guarantee the robustness for disturbance attenuation and uncertainties. Figure 7 shows the block diagram of full state feedback H_∞ control. M_δ is the coefficient matrix for structured uncertainty [17].

$$M_\delta = \begin{bmatrix} A & B_{\delta 1} & B_2 \\ C & D_{11} & D_{\delta 12} \\ C_{\delta 2} & D_{\delta 21} & 0 \end{bmatrix} \quad (39)$$

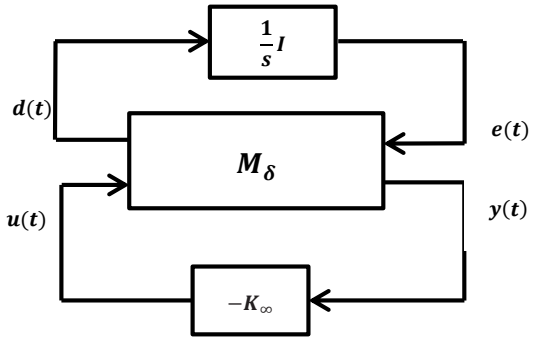

Figure 7: Block diagram of two part system with controller and uncertainty [17].

The stabilizing H_∞ optimal control is obtained such that the infinite norm of the overall closed loop transfer matrix T_{ed} is minimized, that is [16]:

$$\|T_{ed}\|_\infty < \gamma \quad (40)$$

where γ represents a positive integer number.

The objective function for H_∞ optimal control is [17]:

$$J(e,d) = \int_0^\infty (e^T(t)e(t) - \gamma^2 d^T(t)d(t))\, dt \quad (41)$$

$$\inf_u \sup_d J(u,d) < \infty \quad (42)$$

where *inf* represents infinimum and *sup* represents supremum. The optimal state worst case disturbance feedback $d(t)$ is given by [18]:

$$d(t) = K_d\, x(t) \quad (43)$$

Substituting equation (22) in equation (41) yields:

$$J(x(t),t) = \int_0^\infty x^T(t)(Q + K^T K - \gamma^2 {K_d}^T K_d)x(t)\, dt \quad (44)$$

A constant positive semidefinite symmetric matrix P that satisfies equation (42) is supposed to be found, then:

$$\int_0^\infty x^T(t)\left(Q + K^T K - \gamma^2 {K_d}^T K_d\right) x(t) = \int_0^\infty -\frac{d}{dx}\left(x^T(t) P\, x(t)\right) \quad (45)$$

Reformulating equation (45), yields:

$$(A + B_1 K_d + B_2 K)^T P + P(A + B_1 K_d + B_2 K) + {C_1}^T C_1 + K^T K - \gamma^2 {K_d}^T K_d = 0 \quad (46)$$

The condition for maximization of $J(x(t),t)$ with respect to K_d is [18]:

$$\nabla_{K_d} P = 0 \quad (47)$$

The gradient matrix $\nabla_{K_d} P$ is defined as:

$$\left(\nabla_{K_d} P\right)_{ij} = \frac{\partial P}{\partial {K_d}_{ij}} \quad (48)$$

then

$$K_d = -\frac{1}{\gamma^2} {B_1}^T P \quad (49)$$

Similarly, the condition for minimization of $J(x(t),t)$ in equation (46) with respect to K is [18]:

$$K = -{B_2}^T P \quad (50)$$

Substituting equations (49) and (50) in equation (46), the Riccati resulting equation is:

$$PA + A^T P + {C_1}^T C_1 + P\left(B_2 {B_2}^T - \frac{1}{\gamma^2} B_1 {B_1}^T\right) P = 0 \quad (51)$$

On the other hand, to achieve the criterion in equation (56), the following conditions should be satisfied: $u(t) = K\, u(t)$, $P \geq 0$ *and the matrix* $(A + B_1 K_d + B_2 K_c)$ *is stable.*

5. Results and Discussion

The eigenvalues values of the uncontrolled system are $\{0, 0, -10.9719, 10.9719, 0, 0\}$ which indicate the system instability. The H_2 controller is proposed to ensure the stability for the system. Figure 8 illustrates the time response with H_2 controller in case of stabilization. It is clear that the proposed H_2 controller can achieve the stability within 4 $seconds$ and the pendulum angle oscillates between -0.92 to 0.35 $degree$. The resulting control signals are shown in Figure 9. The resulting state feedback gains are:

$$K_2 = \begin{bmatrix} -1.1181 & -1.4113 & 0.7906 & 0.7916 & -5.3592 & -1.2632 \\ -1.1181 & -1.4113 & -0.7906 & -0.7916 & -5.3592 & -1.2632 \end{bmatrix}$$

and the new closed loop eigenvalues are:$\{-2.273 + 1.784\, i,\ -2.273 - 1.784\, i, -1.395, -1, , -1070.739, -733.323\}$ which means that the system, became stable. In this work, the appropriate values of Q_f, N_f and R_f are set by trial and error to be:

$$Q_f = \begin{bmatrix} 200 & 0 & 0 & 0 & 0 & 0 \\ 0 & 100 & 0 & 0 & 0 & 0 \\ 0 & 0 & 100 & 0 & 0 & 0 \\ 0 & 0 & 0 & 100 & 0 & 0 \\ 0 & 0 & 0 & 0 & 100 & 0 \\ 0 & 0 & 0 & 0 & 0 & 100 \end{bmatrix},\ R_f = 80$$

$$N_f = \begin{bmatrix} 1 & 0 & 0 & 0 & 0 & 0 \\ 0 & 0 & 0 & 0 & 0 & 0 \end{bmatrix}.$$

Moreover, it is apparent that the control signal is within the allowable range of the input voltage of the system. Figure 10 shows the system states trajectories. From this figure, it can be observed that the system states trajectories with full state feedback H_∞ controller approach the equilibrium within 5 $sec.$ for system position, 4 $sec.$ for pendulum angle and 4 $sec.$ for rotating angle. Regarding to the deviation of the pendulum angle, it is seen that this angle deviates between -0.47 and 0.1 $degree$. The resulting state feedback gains are:

$$K_c = \begin{bmatrix} -0.0123 & -0.0246 & 0.0138 & 0.0148 & -0.2374 & -0.0314 \\ -0.0123 & -0.0246 & -0.0138 & -0.0148 & -0.2374 & -0.0314 \end{bmatrix}$$

and

$$K_d = \begin{bmatrix} 7.493e^{-10} & 5.111e^{-10} & 1.740e^{-21} & 2.201e^{-22} & 9.563e^{-10} & 1.799e^{-10} \\ 0 & 0 & 0 & 0 & 0 & 0 \end{bmatrix}$$

The new closed loop eigenvalues are: $\{-23.66, -5.279, -0.97 + 0.403i, -0.97 - 0.403i, -12.746, -1.003\}$. This means that all the roots of the system lie in the left hand side and the system is stable.

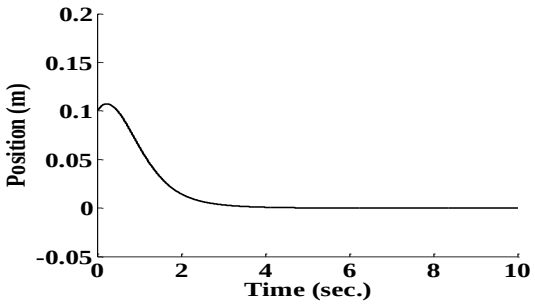

(a)

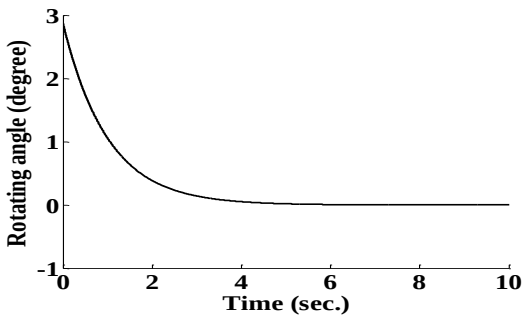

(b)

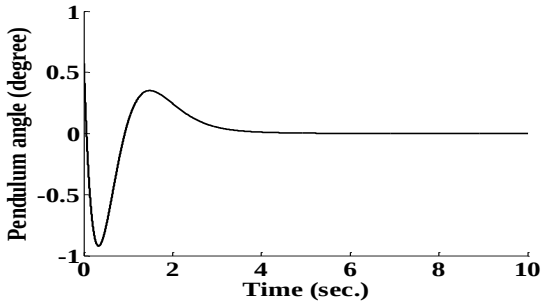

(c)

Figure 8: System state trajectories using H_2 stabilizing controller $x_0 = [0.1 \;\; 2.865 \;\; 0.573]$ a) position b) rotating angle c) pendulum angle d) u_1 e) u_2.

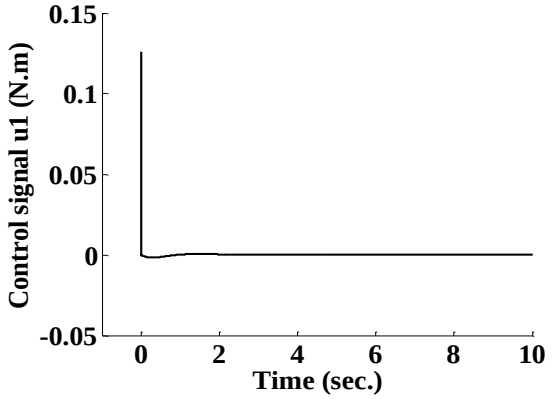

(a)

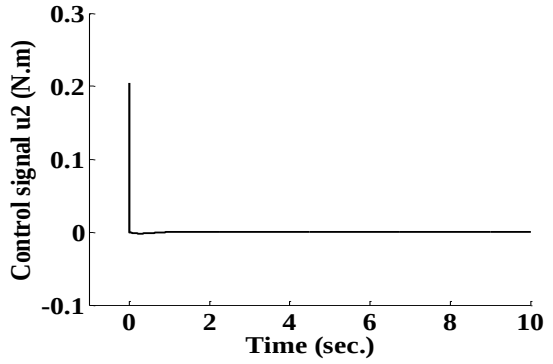

(b)

Figure 9: The resulting control signals using H_2 stabilizing controller a) u_1 and b) u_2.

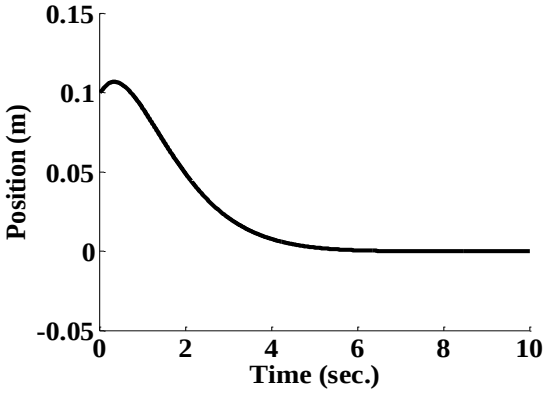

(a)

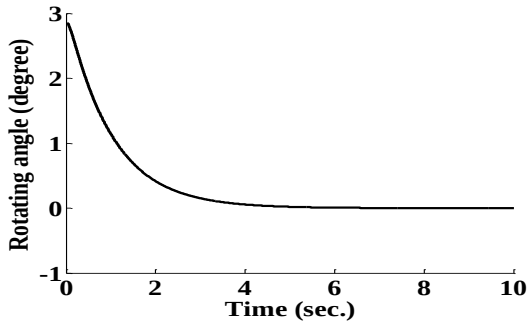

(b)

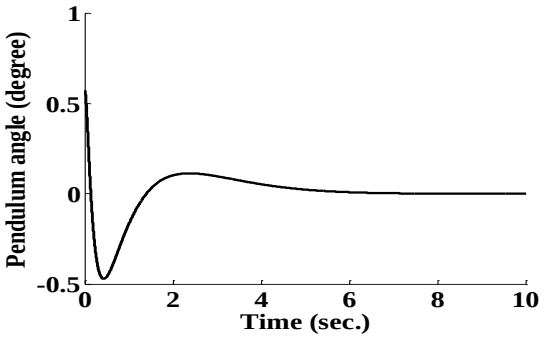

(c)

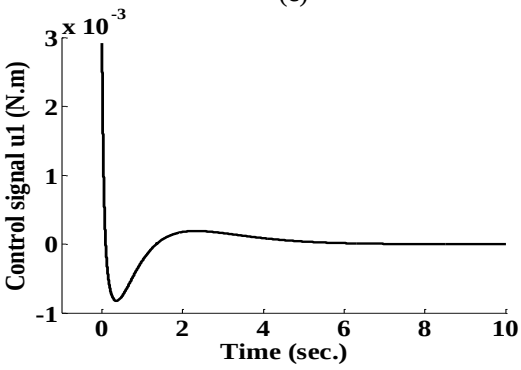

(d)

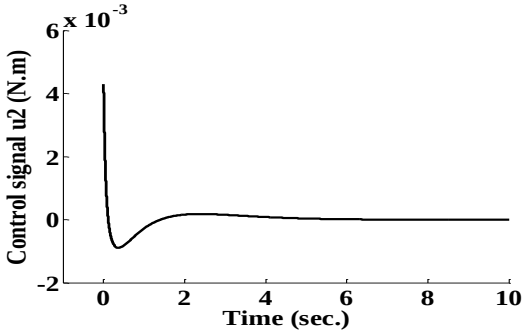

(e)

Figure 10: System state trajectories using H_∞ stabilizing controller $x_0 = [0.1 \;\; 2.865 \;\; 0.573]$, a) position, b) rotating angle, c) pendulum angle, d) u_1 and e) u_2.

Furthermore, Figure 11 shows the system tracking properties using H_∞ controller. The time response characteristics can be summarized by: $t_s = 5\,sec.$ for system position, $t_s = 5\,sec.$ for rotating angle and for pendulum angle the settling time is $6.5\,sec.$ and the pendulum deviates between -1.073 and 3.955 *degree*. Further, it is shown that a low control effort has been resulted and within the allowed range of input torque. Figure 12 gives the time response specifications of the controlled system when the system parameters are changed. Comparisons between the results of H_2 controller and H_∞ in both stabilizing and tracking cases are shown in Figure 13 and 14. The comparison shows that the two controllers yielded relatively the same time response specifications in case of system position, but in case of pendulum angle deviation, it is noted that the full state feedback H_∞ controller is much improved over that of the full state feedback H_2 controller. In addition, the H_∞ controller yielded a very low control signal when it is compared to H_2 controller. These improvements can be attributed to the effectiveness of the H_∞ control method in attenuating the disturbances and resulting a low control signal and within the allowed tolerance to avoid the saturation problem. Add to all, the full state feedback H_∞ controller can compensate the system parameters uncertainty.

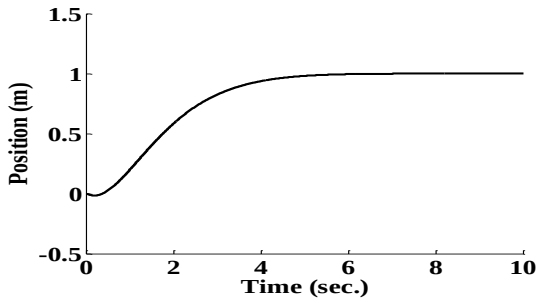

(a)

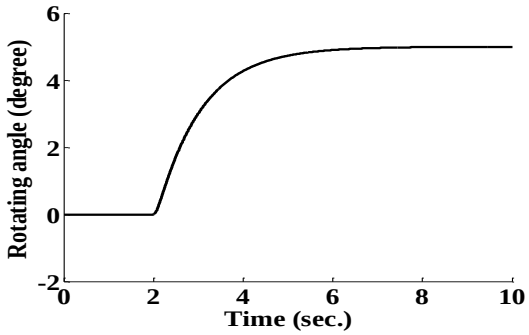

(b)

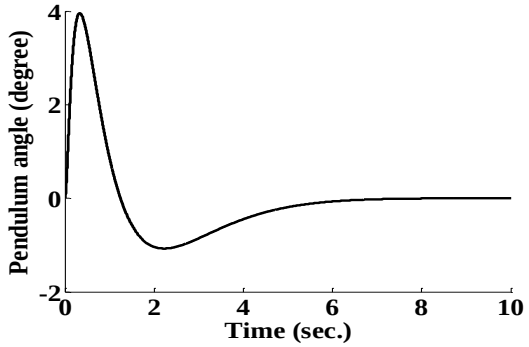

(c)

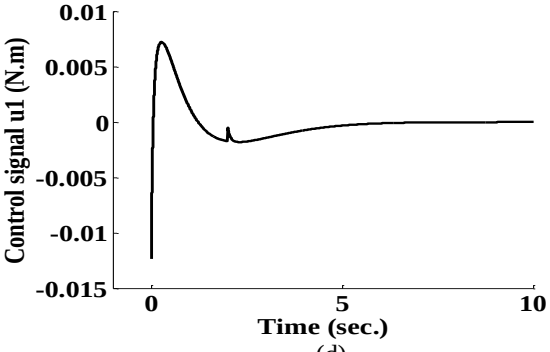

(d)

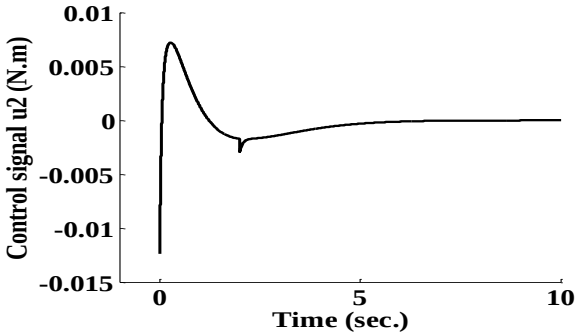

(e)

Figure 11: Tracking properties of the system using H_∞ controller, a) position, b) rotating angle, c) pendulum angle, d) u_1 and e) u_2.

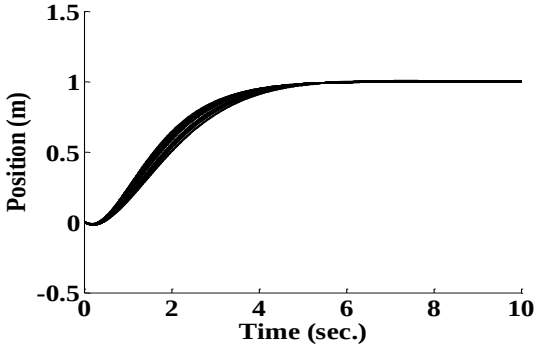

(a)

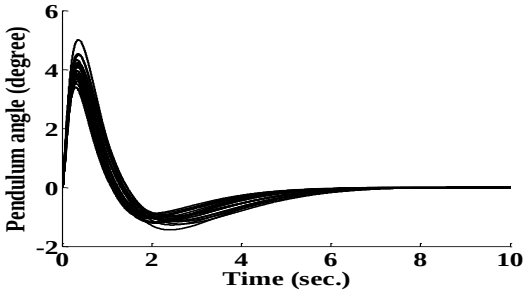

(b)

Figure 12: System time response with parameters uncertainty using H_∞ controller, a) position, b) pendulum angle.

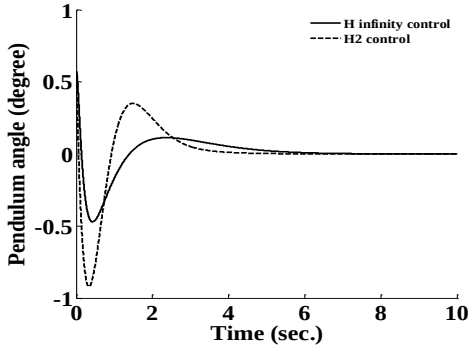

Figure 13: System state trajectory using H_2 stabilizing controller (dotted line) and H_∞ controller (solid line).

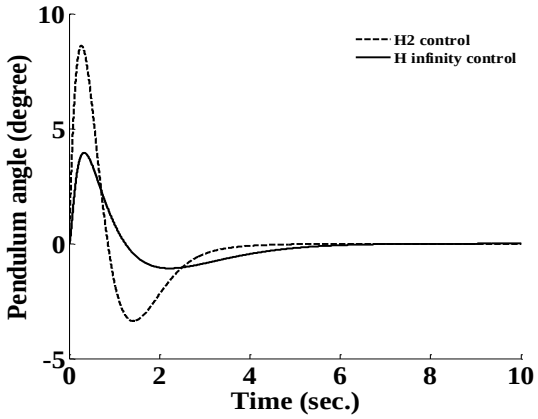

Figure 14: System state trajectory using H_2 controller (dotted line) and H_∞ controller (solid line).

The experimental results for applying a full state feedback H_2 controller as a stabilizing controller are shown in Figure 15. It is shown that the position needs 5 $sec.$ to settle from the downward position to the upright position within -0.04 to 0.04 $degree$ and the pendulum angle deviation is from 0.16 to -0.05 $degree$. The amplitudes of this control action are -0.5 to -0.4 $volt$ which are within the limits of input torques. The experimental results for applying the full state feedback H_∞ controller are shown in Figure 16. It is shown that the position needs 5 $sec.$ to settle from the downward position to the upright position within -0.05 to 0.0473 $degree$ and the pendulum angle deviation is from -0.005 to 0.01 *degree*. The amplitudes of the control action are 0.76 to -0.01 $volt$ which are within the limits of input voltages.

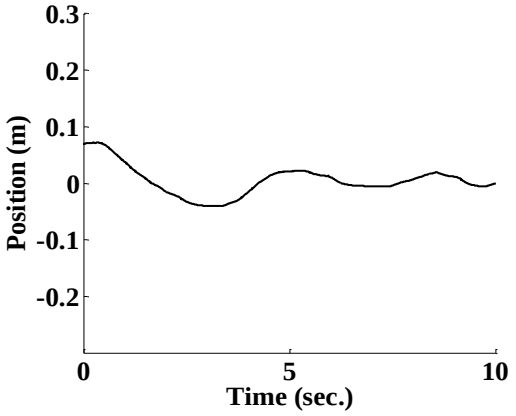

(a)

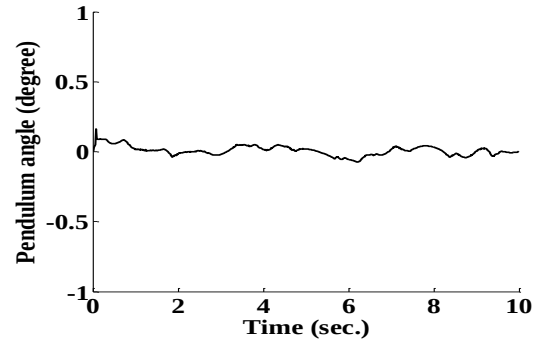

(b)

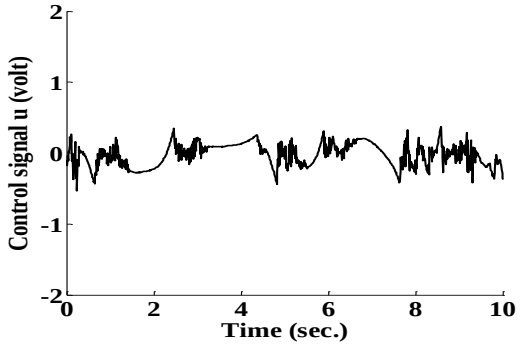

(c)

Figure 15: Experimental response using H_2 stabilizing controller, a) position, b) pendulum angle, c) control signal.

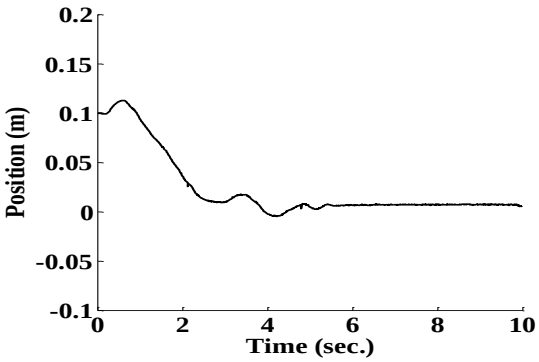

(a)

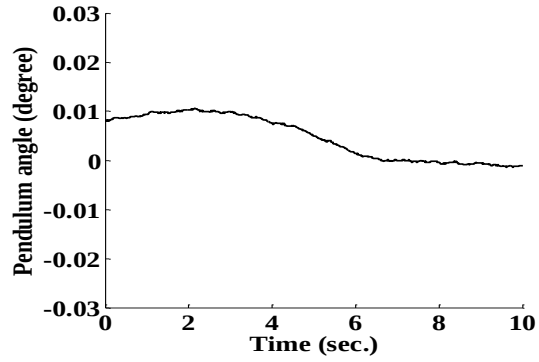

(b)

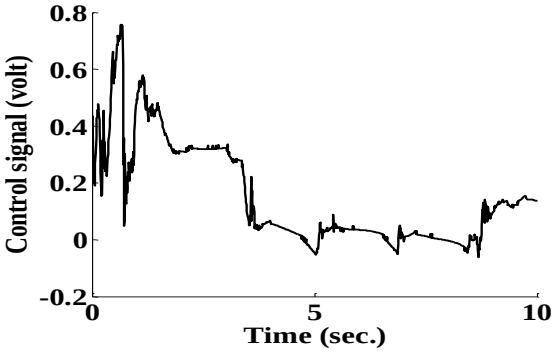

(c)

Figure 16: Experimental time response using H_∞ stabilizing controller, a) position, b) pendulum angle, c) control signal.

Furthermore, the experimental results for applying the full state feedback H_∞ controller as a tracking controller are shown Figure 17. The obtained time response specifications are: $t_s = 5\ sec.$ for system position and for pendulum angle the settling time is $5\ sec.$ and the pendulum deviates between -0.05 and 1.35 *degree*. Further, it is shown that a low control effort has been resulted which is within the allowed range of input torque.

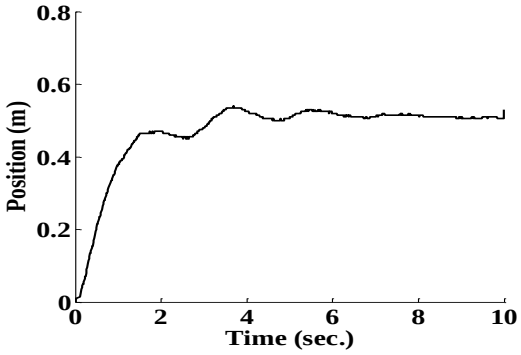

(a)

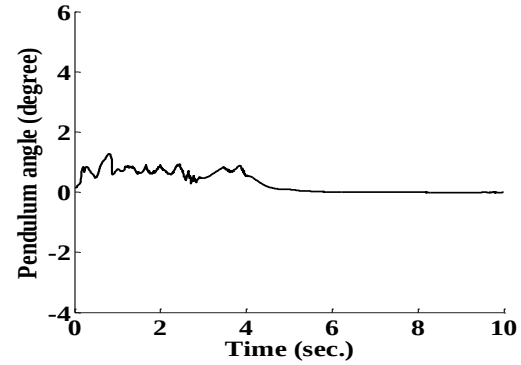

(b)

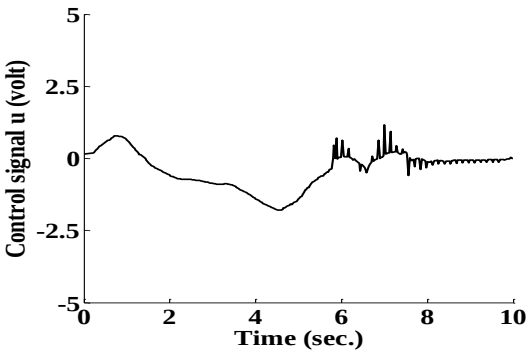

(c)

Figure 17: Experimental time response using H_∞ tracking controller, a) position, b) pendulum angle, c) control signal.

5. Conclusion

The H_2 controller is a powerful technique to design a robust control for rejecting the disturbance and achieving an acceptable time response specifications. The full state feedback H_∞ control is a powerful robust control technique to design a robust control with the presence of disturbance and uncertainties. The robust stability and performance of the system have been assured using the full state feedback H_∞ controller. This controller could achieve time response specifications better than those obtained using H_2 control in addition to a low control effort. The results verified that the proposed state feedback controller using H_∞ technique can stabilize the system and achieve the desirable performance despite the presence of uncertainty. Moreover, it has been shown that a very small deviation in pendulum angle was achieved using the proposed controller in comparison to the controllers designed in previous works. The experimental results showed the superiority of the full state feedback H_∞ controller.

References

[1] A. Ghaffari, A. Shariati and A. H. Shamekhi, "A Modified Dynamical Formulation for Two-Wheeled Self-Balancing Robots," Nonlinear Dynamics, Springer, Vol. 83, No. 1, pp. 217–230, 2016.

[2] M. Yue, X. Wei and Z. Li, "Adaptive Sliding Mode Control for Two-Wheeled Inverted Pendulum Vehicle Based on Zero Dynamics Theory," Nonlinear Dynamics, Springer, Vol. 76, No. 1, pp. 459-471, 2013.

[3] A. Bature, S. Buyamin, N. Ahmad and M. Muhammad "A Comparison of Controllers for Balancing Two Wheeled Inverted Pendulum Robot," International Journal of Mechanical & Mechatronics Engineering, IJMME-IJENS, Vol.14, No.3, pp. 62-68, 2014.

[4] J. Huang, Z. H. Guan, T. Matsuno, T. Fukuda, and K. Sekiyama, "Sliding Mode Velocity Control of Mobile Wheeled Inverted Pendulum Systems," Transactions on Robotics, IEEE, Vol. 26, No. 4, pp. 750–758, 2010.

[5] C. Xu, M. Li and F. Pan, "The System Design and LQR Control of a Two Wheel Self Balancing Mobile Robot," International Conference on Electrical and Control Engineering (ICECE), IEEE, China, 2011.

[6] F. Liu, S. Cao and Y. Li, " PD Backstepping Controller for Stabilization of Wheeled Inverted Pendulum," Proceedings of the 〖34〗^th Chinese Control Conference, China, 2015.

[7] Y. S. Zhou and Z. H. Wan, "Robust Motion Control of a Two-Wheeled Inverted Pendulum with an Input Delay Based on Optimal Integral Sliding Mode Manifold," Nonlinear Dynamics, Springer, Vol. 85, No. 3, pp. 2065–2074, 2016.

[8] W. S. Levine, "Control System Fundamentals", CRC press LLC, 2011.

[9] R. M. Brisilla and V. Sankaranarayanan, "Nonlinear control of mobile inverted pendulum," Robotics and Autonomous Systems, Vol. 70, No. 4, pp. 145–155, 2015.

[10] M. Yue, C. An, Y. Du and J. Sun, " Indirect Adaptive Fuzzy Control for a Nonholonomic Underactuated Wheeled Inverted Pendulum Vehicle Based on a Data-Driven Trajectory Planner," Fuzzy Sets and Systems, Vol. 290, No.1, pp. 158–177, 2015.

[11] Y. Zhou and Z. Wang, "Motion Controller Design of Wheeled Inverted Pendulum with an Input Delay Via Optimal Control Theory," Journal of Optimization Theory and Applications, Springer, Vol. 168, No. 2, pp. 625-645, 2016.

[12] A. Sinha, P. Prasoon, P. K. Bharadwaj and A. C. Ranasinghe, "Nonlinear Autonomous Control of a Two-Wheeled Inverted Pendulum Mobile Robot Based on Sliding Mode," International Conference on Computational Intelligence & Networks, IEEE, India, 2015.

[13] http://www.sainsmart.com.

[14] C. Fauvel, F. Claveau and P. Chevrel, "A Generically Well-Posed H_2 Control Problem for a One Shot Feedforward and Feedback Synthesis," 17th International Conference System Theory, Control and Computing (ICSTCC), IEEE, pp. 201 - 206, 2013.

[15] X. H. Chang, "Robust Output Feedback H-infinity Control and Filtering for Uncertain Linear Systems," Springer Heidelberg, London, 2014.

[16] Z. Kemin and D. Jhon, "Essentials of Robust Control," Upper Saddle River, New Jersey: Prentice Hall Inc., 1998.

[17] H. Wu and B. Luo, "Simultaneous Policy Update Algorithms for Learning the Solution of Linear

Continuous Time H_∞ state feedback control," Information Sciences, Vol. 222, pp. 472-485, 2013.

[18] A. Sinha, "Linear Systems Optimal and Robust Control," Taylor & Francis Group, New York, 2007.

Author's biography

Hazem. I. Ali

He graduated from the department of Control and Systems Engineering, University of Technology, Baghdad, Iraq in 1997. He obtained the MSc degree in Mechatronics Engineering from University of Technology, Baghdad, Iraq in 2000 and the PhD in Control and Automation from the Department of Electrical and Electronics Engineering, University Putra Malaysia, Malaysia in 2010. Currently he is an Assistant Professor in Control and Systems Engineering Department, University of Technology, Baghdad, Iraq. His current research interests include robust control, intelligent control and optimization techniques. He is a member of IEEE and IAENG.

Zain. M. Shareef

He graduated from the department of Control and Systems Engineering, University of Technology, Baghdad, Iraq in 2013. He obtained the MSc degree in Control Engineering from University of Technology, Baghdad, Iraq in 2016. His current research interests include robust control and intelligent control.